8

Optimal Signal Design for Wavelet Radio TOA Locationing with Synchronization Error for 5G Networks

Homayoun Nikookar

Netherlands Defence Academy, the Netherlands

8.1 Introduction

High throughput and low cost and latency as well as high reliability, spectral efficiency and flexibility are, among others, major requirements of 5G. Another remarkable issue for the 5G networks is its context-awareness. Context can be location. Location-based services are becoming more and more important. In this chapter accurate positioning of devices with 5G using flexible wavelet packet modulation is addressed. Wavelet Packet modulated (WPM) signal can be used for joint communications and ranging (two functionalities in one technology). Using wavelet technology the optimal signal will be designed for the time-of-arrival (TOA) or time-difference-of-arrival (TDOA) locationing when there exists a synchronization error. The focus will be on the wavelet packet modulated signal as wavelets have lower sensitivity to distortion and interference as a result of synchronization error. Further advantage of wavelet technology lies in its flexibility to customize and shape the characteristics of the waveforms for 5G radio communication and ranging purposes. In addition to the flexibility, the reconfigurability of the wavelet signals is also an important characteristic for the successful application of this technology in cognitive radio communication and ranging systems.

There are basically three methods to estimate the position with radio signals: Received Signal Strength (RSS), Angle of Arrival (AOA) and Time of Arrival (TOA) [1, 2]. Here we focus on the TOA method. In this location technique the time of arrival of the signal sent by the mobile agent to be positioned is measured at each receiver (access point). The propagation time of each signal is known and is proportional to the distance. As shown in Figure 8.1 the measured time provides information in a set of points around the circumference of a circle having the radius of distance between the object (mobile) and the access point. The intersection of the circles is the mobile's position. Similar to the RSS method, for the 2-D location based on the TOA technique, at least three access points are required. Let t_1, t_2 and t_3 denote the flight time of the transmitted signal of the object (mobile) to be positioned, to the respective receivers (access points). The access points 1, 2 and 3 are respectively positioned at locations (0,0), $(0,y_2)$ and (x_3,y_3). Let (x,y) denote the coordinates of the handset (object) to be positioned. By estimating the time of arrivals, the following set of equations should be solved to obtain the position (x,y) of the mobile devices.

$$\begin{aligned} d_1 &= ct_1 = \sqrt{x^2 + y^2} \\ d_2 &= ct_2 = \sqrt{x^2 + (y - y_2)^2} \\ d_3 &= ct_3 = \sqrt{(x - x_3)^2 + (y - y_3)^2} \end{aligned} \tag{8.1}$$

where c is the speed of light. It should be mentioned that to avoid ambiguity in identifying the intersection of circles in Figure 8.1 all three equations in (8.1) must be considered.

The key factor in time based distance estimator is the arrival time of the first path. TOA utilizes the time delay to get the distance and looks for the intersection of at least three circles to estimate the location. It requires synchronization at both transmitter and receiver side, which is always an important issue in the wireless network, as well as the information of transmission time. If the system is not synchronized or if there is an offset in the time of transmission, the TOA methods cannot work properly. For instance, even a 1msec inaccuracy in the TOA estimation can cause an error of up to 300 m in ranging!

A variant of TOA, the time difference of arrival (TDOA) scheme, can improve the situation. It calculates the target mobile's position according to the time differences between each measurements, rather than the time measurement itself as in TOA. Therefore, as shown in Figure 8.2, the TDOA searches the hyperbolic intersection and only needs the receiver clock synchronization without the information of time of transmission. The equations for the TDOA positioning become:

$$\begin{aligned} &\sqrt{(x - x_i)^2 + (y - y_i)^2} - \sqrt{(x - x_j)^2 + (y - y_j)^2} = d_i - d_j, \\ &i = 1,2,3 \quad \text{and} \quad j = 1,2,3 \end{aligned} \tag{8.2}$$

Efficient methods to solve these nonlinear equations have been reported [3].

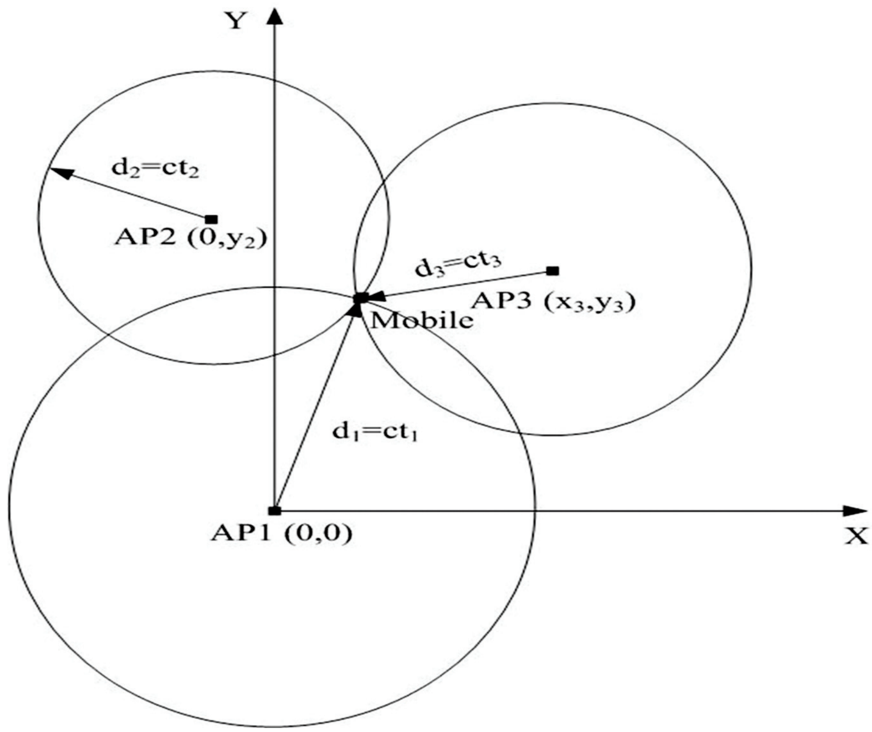

Figure 8.1 The TOA positioning method (APi: *i*th Access Point).

The RSS method is not an accurate method in locationing, especially in multipath fading environments. The AOA method requires a complex hardware. The TOA and TDOA methods are more appropriate for the positioning (especially when the bandwidth of the transmission is wide providing a fine time resolution). A remarkable issue in locationing with the TOA or TDOA techniques is the estimation of the arrival time of the transmitted signals. Major TOA estimation techniques use the correlation function and find its maximum to estimate the TOA or TDOA [4].

In this chapter we shall design the optimal signal for TOA or TDOA locationing when there exists a synchronization error. We particularly concentrate on the wavelet packet modulated signal for communications and ranging[1] as wavelets have lower sensitivity to distortion and interference (due to

[1] It should be emphasized that the Wavelet Packet Modulated (WPM) signal can be used for joint communications and ranging. This joint functionality in one technology is the outstanding capability of the WPM signal.

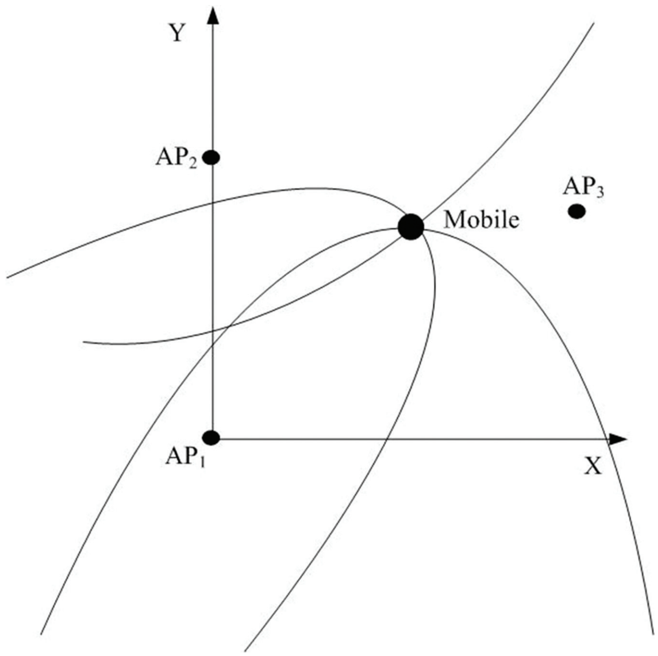

Figure 8.2 The TDOA positioning method (APi: *i*th Access Point).

synchronization error) and also provide flexibility in signal design when there exists a synchronization error in the received signal. The advantage of wavelet transform lies in its flexibility to customize and shape the characteristics of the waveforms for radio communication and ranging purposes. In addition to the flexibility, the reconfigurability of the wavelet signals is also an important characteristic of this technology which paves the way for its successful application in cognitive radio communication and ranging systems of future.

8.2 Wavelet Signal Design

This Section focuses on the design steps of wavelet signal. The implementation of filter also will be discussed in this section.

8.2.1 Design Procedure

The attributes of the wavelet packet modulation system greatly depend on the set of transmission bases utilized which in turn is determined by the filters used. This means that by adapting the filters one can adapt the transmit waveform characteristics to satisfy a system specification. Choosing the right filter though is a delicate task. The filters cannot be arbitrarily chosen and instead have to satisfy a number of constraints. Besides the design objectives there are other budgets which have to be considered in order to guarantee that the designed wavelet is valid. The design procedure consists of 3 major steps [5], namely:

1. Formulation of design problem, i.e., stating the design objectives and constraints mandated by wavelet theory.
2. Application of suitable optimizations and transformations to make the problem tractable.
3. Utilization of numerical solvers to obtain the required filter coefficients.

At the end of the design procedure a low pass Finite-Impulse-Response (FIR) filter $h[n]$, satisfying the design and wavelet constraints, is obtained. From this filter the other three filters $g[n]$, i.e., the high-pass filter, $h'[n]$, i.e., the dual of $h[n]$ and $g'[n]$, i.e., the dual of $g[n]$ are derived through the Quadrature Mirror Filter (QMF) relation [5], i.e., $g[n] = (-1)^n h[L-1-n]$, for $h[n]$ of length L. Where $h'[n] = h^*[-n]$, and $g'[n] = g^*[-n]$.

In the following sections we will elaborate on each of these processes.

8.2.2 Filter Bank Implementation of Wavelet Packets

It is well known that compactly supported orthonormal wavelets can be obtained from a tree structure constructed by successively iterating discrete two-channel paraunitary filter banks [5–8]. Time and frequency limited orthonormal wavelet packet bases $\xi(t)$ can be derived by recursively iterating discrete half-band high $g[n]$ and low-pass $h[n]$ filters, as[2]:

$$\begin{aligned} \xi_{l+1}^{2p}(t) &= \sqrt{2}\sum_m h\,[m]\,\xi_l^p\,(2t-m) \\ \xi_{l+1}^{2p+1}(t) &= \sqrt{2}\sum_m g\,[m]\,\xi_l^p\,(2t-m) \end{aligned} \tag{8.3}$$

In (8.3) the subscript l denotes the level in the wavelet tree structure and superscript p indicates the waveform index.The number of bases p generated is determined by the number of iterations l of the two-channel filter bank. Equation (8.3), known as 2-scale equation, can be interpreted as follows – a basis function belonging to a certain subspace of lower resolution can be obtained from shifted versions of the bases belonging to a subspace of higher resolution; and the weights h and g used in the transformation are low and high pass in nature. The filters h and g form a quadrature mirror pair and are also known as analysis filters. These filters have duals/adjoints known

[2]The expressions are considered in continuous time domain to convenience derivations in Section 8.4.

as synthesis filters which are also a pair of half-band low h' and high pass filters g'. All these four filters share a strict and tight relation and hence it is enough if the specifications of one of these filters are available. The wavelet packet sub-carriers (used at the radio transmitter end) are generated from the synthesis filters. And the wavelet packet duals (used at the radio receiver end) are obtained from the analysis filters. The entire wavelet packet modulated (WPM) transceiver structure can thus be realized by this set of two QMF pairs. Hence, the design process can also be confined to the construction of one of the filters, usually the low pass analysis filter *h*.

8.3 Problem Statement

The time synchronization error in the received signal for the data detection of communications and the TOA or TDOA estimation of ranging is modeled by shifting the received data samples R[n] by a time offset Δ_t to the left or right as:

$$R[n \pm \Delta_t] = S[n] + w[n]. \tag{8.4}$$

Here, S[n] denotes the transmitted signal and w[n] the additive white Gaussian noise (AWGN). According to wavelet theory [5] under ideal conditions, when the WPM transmitter and receiver are perfectly synchronized and the channel is benign, the detection of signal in the *u*th symbol and *k*th sub-carrier $\hat{a}_{u',k'}$ is the same as the transmitted data $a_{u,k}$[3]. However, errors are introduced in the demodulation decision making process under time offset errors Δ_t as elucidated below:

$$\begin{aligned}
\hat{a}_{u',k'} &= \sum_n R[n] \xi_l^{k'} [(u'N - n + \Delta_t] \\
&= \sum_n \sum_u \sum_{k=0}^{N-1} a_{u,k} \xi_l^k [n - uN] \xi_l^{k'} [u'N - n + \Delta_t] \\
&= \sum_u \sum_{k=0}^{N-1} a_{u,k} \left(\sum_n \xi_l^k [n - uN] \xi_l^{k'} [u'N - n + \Delta_t] \right)
\end{aligned} \tag{8.5}$$

Where *N* is the number of wavelet subcarriers. Defining the cross waveform function $\Omega(\Delta_t)$ as:

$$\Omega_{k,k'}^{u,u'}[\Delta_t] = \sum_n \xi_l^k [n - uN] \xi_l^{k'} [u'N - n + \Delta_t] \tag{8.6}$$

[3]The apostrophes in the symbol u' and carrier k' indices are used to indicate receiver side.

the demodulated data corrupted by the interference due to loss of orthogonality at the receiver for the kth subcarrier and uth symbol can be expressed as:

$$\hat{a}_{u',k'} = \underbrace{a_{u',k'}\Omega^{u',u'}_{k',k'}[\Delta_t]}_{\text{Desired Alphabet}} + \underbrace{\sum_{u;u\neq u'} a_{u,k'}\Omega^{u,u'}_{k',k'}[\Delta_t]}_{\text{ISI}}$$
$$+ \underbrace{\sum_{u}\sum_{k=0;k\neq k'}^{N-1} a_{u,k}\Omega^{u,u'}_{k,k'}[\Delta_t]}_{\text{IS}-\text{ICI}} + \underbrace{w_{u',k'}}_{\text{Gaussian Noise}} \quad (8.7)$$

For the data communication, in (8.7), the first term stands for the attenuated useful signal, the second term denotes Inter Symbol Interference (ISI), third term gives Inter Symbol Inter Carrier Interference (IS-ICI) and the last term stands for Gaussian noise. Generally speaking multi-carrier systems are highly sensitive to loss of time synchronization. A loss of time synchrony results in samples outside a WPM symbol getting selected erroneously, while useful samples at the beginning or at the end of the symbol getting discarded. It also introduces ISI and ICI causing performance degradation.

For the locationing, TOA or TDOA estimation methods use the correlation function and find its maximum to estimate the time of arrival of the signal to be used for positioning. However, because of time synchronization error there will be a cross correlation energy between the wavelets. Therefore, our objective in this paper is to design proper wavelets for TOA ranging when there is a time synchronization error. The design is achieved by minimizing the interference caused by the timing error.

We also note that though WPM and Orthogonal Frequency Division Multiplexing (OFDM) share many similarities as orthogonal multicarrier systems, they are significantly different in their responses to loss of time synchronization. This difference is a result of the fact that the WPM symbols overlap with each other and are longer than the OFDM symbol[4]. Under a loss in time synchronization, the overlap of the symbols in WPM causes each symbol to interfere with several other symbols while in OFDM each symbol interferes only with its neighbors. The second important difference is in the usage of guard intervals. OFDM benefits from the cyclic prefix which significantly improves its performance under timing errors. WPM cannot use guard intervals because of the symbol overlap.

[4]The length of the symbol and the degree of overlap is determined by the length of wavelet filter used.

Fortunately, WPM offers the possibility in adjusting the properties of the waveforms in a way that the errors due to loss of synchronization can be minimized. In Section 8.5 we present a method to design a new family of wavelet filters which minimize the energy of the timing error interference for ranging applications. But before that, let us discuss the major wavelet properties that are important in the selection of wavelets.

8.4 Important Wavelet Properties

Generally speaking the wavelet tool is a double edged sword – on one hand there is scope for customization and adaptation; on the other hand there are no clear guidelines to choose the best wavelet from for a given application. In order to ease the selection process constraints, such as orthogonality, compact support and smoothness are imposed. Here we shall discuss them in more detail.

8.4.1 Wavelet Existence and Compact Support

This constraint is necessary to ensure that the wavelet has finite non-zero coefficient and thus the impulse response of the wavelet decomposition filter is finite as well. According to [9], this property can be derived by simply integrating both sides of the two-scale Equation in (8.8) and can be derived as follows[5]:

$$
\begin{aligned}
\int_{-\infty}^{\infty} \xi(t)dt &= \sqrt{2}\int_{-\infty}^{\infty} \sum_n h[n]\xi(2t-n)dt \\
\int_{-\infty}^{\infty} \xi(t)dt &= \sqrt{2}\sum_n h\,[n] \int_{-\infty}^{\infty} \xi(2t-n)dt \\
\int_{-\infty}^{\infty} \xi(t)dt &= \sqrt{2}\sum_n h\,[n] \int_{-\infty}^{\infty} 0.5\xi(2t-n)d(2t-n)
\end{aligned}
\tag{8.8}
$$

Substituting $u = 2t - n$, (8.8) can be rewritten as:

$$
\begin{aligned}
\int_{-\infty}^{\infty} \xi(t)dt &= \frac{1}{\sqrt{2}}\sum_n h\,[n] \int_{-\infty}^{\infty} \xi(u)du \\
\frac{\int_{-\infty}^{\infty} \xi(t)dt}{\int_{-\infty}^{\infty} \xi(u)du} &= \frac{1}{\sqrt{2}}\sum_n h\,[n]
\end{aligned}
$$

[5]The subscripts denoting the decomposition level l and the waveform index p have been dropped for convenience.

Finally we obtain the compactly supported wavelet constraint as:

$$\sum_n h[n] = \sqrt{2} \tag{8.9}$$

It should be noted that the derivation resulting in (8.9) is also recognized as the wavelet existence constraint.

8.4.2 Paraunitary Condition

The paraunitary or the orthogonality condition is essential for many reasons. First, it is a prerequisite for generating orthonormal wavelets [6, 7]. Second, it automatically ensures perfect reconstruction of the decomposed signal. The constraint can be derived using the orthonormality property of the scaling function and its shifted version as follows:

$$\int_{-\infty}^{\infty} \xi\,(t)\,\xi\,(t-k)\,dt = \delta[k] \tag{8.10}$$

Substituting the two-scale Equation (8.3) in (8.10) we get:

$$\int_{-\infty}^{\infty} \sum_n h\,[n]\,\xi(2t-n)\sqrt{2} \sum_m h\,[m]\,\xi(2(t-k)-m)\sqrt{2}dt = \delta[k]$$

$$2\sum_n h\,[n] \sum_m h\,[m] \int_{-\infty}^{\infty} \xi(2t-n)\xi(2(t-k)-m)dt = \delta[k]$$

$$2\sum_n h\,[n] \sum_m h\,[m] \int_{-\infty}^{\infty} 0.5\xi(2t-n)\xi(2(t-k)-m)d(2t) = \delta[k] \tag{8.11a}$$

Or

$$\sum_n h\,[n]\,h\,[n-2k] = \delta[k] \quad \text{for } k = 0, 1, \ldots, (L/2)-1 \tag{8.11b}$$

Equation (8.11b) is called double shift orthogonality relation of the wavelet low pass filters impulse responses. In (8.11b), L illustrates the length of the low pass wavelet filter impulse response. For a filter of length L the orthogonality condition (8.11b) imposes $^{L}/_{2}$ non-linear constraints on $h[n]$.

8.4.3 Flatness/*K*-Regularity

This property is a rough measure of smoothness of the wavelet. The regularity condition is needed to ensure that the wavelet is smooth in both time and frequency domains [10]. It is normally quantified by the number of times a wavelet is continuously differentiable. The simplest regularity condition is the *flatness* constraint which is stated on the low pass filter. A low pass filter (LPF), $h[n]$, is said to satisfy Kth order flatness if its transfer function $H(\omega)$ contains K zeroes located at the Nyquist frequency ($\omega = \pi$). For any function $Q(\omega)$ with no poles or zeros at ($\omega = \pi$) this can be written as:

$$H(\omega) = \left(\frac{1 + e^{j\omega}}{2}\right)^K Q(\omega) \quad \text{with } Q(\pi) \neq 0 \tag{8.12}$$

In (8.12), $Q(\omega)$ is a factor of $H(\omega)$ that does not have any single zero at $\omega = \pi$. Having K number of zeros at $\omega = \pi$ also means that $H(\omega)$is K-times differentiable and its derivatives are zero when they are evaluated at $\omega = \pi$. Considering that:

$$H(\omega) = \sum_n h[n] \exp(-j\omega n), \tag{8.13}$$

the kth order derivative of $H(\omega)$ would be:

$$H^{(k)}(\omega) = \sum_n h[n] (-jn)^k \exp(-j\omega n) \tag{8.14}$$

The evaluation of (8.14) at $\omega = \pi$ would result in:

$$\begin{aligned} H^{(k)}(\pi) &= \sum_n h[n] (-jn)^k \exp(-j\pi n) \\ \sum_n h[n] (-j)^k (n)^k (e^{-j\pi})^n &= 0 \\ \sum_n h[n] (-1)^n (n)^k &= 0 \end{aligned}$$

Therefore, the K-regularity constraint in terms of the low pass filter coefficients can be given as:

$$\sum_n h[n] (n)^k (-1)^n = 0 \quad \text{for } k = 0, 1, 2, \ldots, K-1 \tag{8.15}$$

8.4.4 Degrees of Freedom to Design

The criterion (8.9), (8.11b) and (8.15) are necessary and sufficient conditions for the set to form an orthonormal basis and these conditions have to be

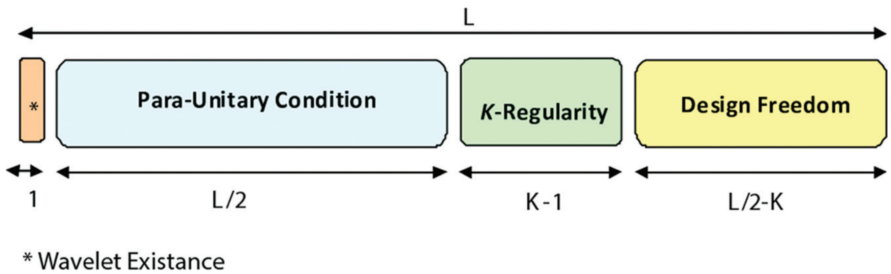

Figure 8.3 Wavelet conditions and degrees of freedom for design.

imposed for all design procedures. For a filter of length L this is essentially getting L unknown filter variables from L equations. Of these L equations, one equation is required to satisfy the wavelet existence condition, $^{L}/_{2}$ come from the paraunitaryness constraint, $K-1$ from the regularity constraint and the remaining $^{L}/_{2}$-K conditions offer the possibility for establishing the design objective. The larger the value of $^{L}/_{2}$-K, the greater the degree of freedom for design and the greater is the loss in regularity. There is therefore a trade-off on offer. The $^{L}/_{2}$-K degrees of freedom that remain after satisfying wavelet existence, orthogonality and K-regularity condition can be used to design a scaling filter with the desired property (refer to Figure 8.3). In the next section we illustrate this with a special signal design example for the ranging application of wavelet packet modulation signal.

8.5 Formulation of Design Problem

In this Section, different aspects for formulation of design problem are discussed. Details on how the mathematical constraints converted from non-convex problem to the convex-problem are presented in this section as well.

8.5.1 Design Criterion

In disturbance-free environments the cross-correlations of WPM waveforms equal zero and perfect reconstruction is possible despite the time and frequency overlap. The timing error Δ_t on the other hand leads to the loss of the orthogonality between the waveforms and consequently they begin to interfere one with another leading to ICI and ISI error for communication and degrading the TOA estimation performance for ranging, stated as:

$$\Omega^{u,u'}_{k,k';k\neq k'}[\Delta_t] = \sum_n \xi^k_l(n-uN)\xi^{k'}_l(u'N-n+\Delta_t) \tag{8.16}$$

The design objective would therefore be to generate wavelet bases ξ and their duals ξ' that minimize interference energy in the presence of timing error:

$$\text{MINIMIZE:} \sum_{u,k;k\neq k'} \left|\Omega^{u,u'}_{k,k'}[\Delta_t]\right|^2 \text{with respect to } \{\xi,\xi'\} \tag{8.17}$$

8.5.2 Wavelet Domain to Filter Bank Domain

The waveforms are created by the multilayered tree structure filter bank. Using Parseval's theorem of energy conservation it can be easily proven that the total energy at each level is equal regardless of the tree's depth. Therefore, minimizing the interfering energy at the roots of the tree will automatically lead to the decrease of total interfering energy at the higher tree branches. Furthermore, the two-channel filter banks through the 2-scale equation are related, albeit explicitly, to the wavelet waveforms. Therefore, the design process can be converted into a tractable filter design problem. We should hence be able to minimize deleterious effects of time synchronization errors in wavelet radio ranging by minimizing the following cross-correlation function:

$$\sum_{\Delta_t} |r_{hg}[\Delta_t]|^2 = \sum_n |h[n]g[n-\Delta_t]|^2 = \sum_n |h[n]((-1)^n h[L-n+\Delta_t])|^2 \tag{8.18}$$

The design problem of minimizing the interference energy due to timing offset can now be formally stated as an optimization problem with objective function (8.18) and constraints (8.9), (8.11b) and (8.15), i.e.,

$$\begin{aligned} \text{MINIMIZE:} & \sum_{\Delta_t} |r_{hg}[\Delta_t]|^2 \quad \text{with respect to } h[n] \\ & \sum_n h[n] = \sqrt{2} \\ \text{SUBJECTTO:} & \sum_n h[n]\,h[n-2k] = \delta[k] \quad \text{for } k = 0,1,\ldots,(L/2)-1 \\ & \sum_n h[n]\,(n)^k(-1)^n = 0 \quad \text{for } k = 0,1,2,\ldots,K-1 \end{aligned} \tag{8.19}$$

As obvious, the second constraint in (8.19) is non-linear and therefore the optimization problem becomes a non-convex one. Thus, the optimization problem as given above can only be solved by general purpose solvers. However, such solvers are susceptible to being trapped in local minima. In order to overcome this difficulty, some authors have suggested multiple starting point techniques or branch-and-bound method [11]. Moreover, general purpose algorithms cannot guarantee that the found result is a global minimum and furthermore when number of constraints increases these algorithms often fail to provide a valid solution. The objective function and constraints can be solved much more efficiently using convex optimization and semi-definite programs [12–18]. In the following sections we attempt to express the design constraints in convex form so that convex optimization tools can be employed to obtain the solution [19–21]. Similar to the wavelet signal design for the distributed radio sensing networks [22], we shall move to the auto-correlation domain $(r_h[k] = \sum_{m \in z} h[m]h[m+k])$ to simplify the minimization problem.

8.5.3 Transformation of the Mathematical Constraints from Non-convex Problem to a Convex/linear One

Fortunately, it is possible to transform the non-convex/non-linear equations into a linear/convex problem by reformulating the constraints in terms of the autocorrelation sequence $r_h[k]$, [23–25]:

$$r_h[k] = \sum_{m \in z} h[m]\, h[m+k] \tag{8.20}$$

Taking into account the inherent symmetry of the autocorrelation sequence it can be defined more precisely as:

$$r_h[l] = \sum_{n=0}^{L-l-1} h[n]\, h[n+l] \quad \text{for } l \geq 0 \tag{8.21}$$

In (8.21), L is the length of the FIR filter and the autocorrelation function is symmetric about $l = 0$; i.e.:

$$r_h[-l] = r_h[l] \tag{8.22}$$

The three constraints (8.9), (8.11b), and (8.15) are derived in terms of $r_h[l]$ in the following sub-sections.

8.5.3.1 Compact support or admissibility constraint

The compact support constraint in (8.3) can be rewritten as:

$$\sum_{n=0}^{L-1} \sum_{l=-n}^{L-n-1} h[n]\, h[n+l] = 2 \tag{8.23}$$

Reversing the order of the summation and considering the fact that the impulse response of filter $h[n]$ has non-zero values only at $0 \leq n \leq L-1$, we obtain:

$$\sum_{l=-(L-1)}^{L-1} \sum_{n=0}^{L-l-1} h[n]\, h[n+l] = 2 \tag{8.24}$$

The compact support constraint in (8.9) can then be rewritten as:

$$\sum_{l=-(L-1)}^{L-1} r_h\,[l] = 2 \tag{8.25}$$

Taking into consideration the double shift orthonormality property (see Equation (8.11b)) and the fact that the autocorrelation sequence is symmetric, we can simplify (8.25) further as:

$$r_h\,[0] + 2\sum_{l=1}^{L-1} r_h\,[l] = 2 \quad \text{or}$$

$$\sum_{l=1}^{L-1} r_h\,[l] = \frac{1}{2} \tag{8.26}$$

Equation (8.26) is the compactly supported wavelet constraint stated in terms of the autocorrelation sequence $r_h[l]$.

8.5.3.2 Double shift orthogonality constraint

The double shift orthogonality constraint presented in (8.11b), can be expressed in terms of the autocorrelation sequence $r_h[l]$ as follows:

$$\sum_{m} h[m]\, h[m+2k] = r_h[2k] = \delta[k] \tag{8.27}$$

It should be noted that (8.27) is obtained by applying $n - 2k = m$ in Equation (8.11b). Hence the final double shift orthogonality constraint in terms of autocorrelation sequence $r_h[l]$ is:

$$r_h[2k] = \delta[k] = \begin{cases} 1, & \text{for } k\ = 0 \\ 0, & \text{otherwise} \end{cases} \quad \text{with } k = 0, 1, \ldots, \left\lfloor \frac{L-1}{2} \right\rfloor \tag{8.28}$$

where $\lfloor \cdot \rfloor$ denotes the floor function or the integer part of $(\cdot)$ which is the greatest integer that is less than or equal to $(\cdot)$. Again we make use of the symmetry property to simplify it. In contrast to (8.11b) which was non-convex, (8.28) consists of linear equalities and is also convex.

8.5.3.3 *K*-Regularity constraint

The regularity constraint can be reformulated in terms of autocorrelation sequence $r_h[l]$ by considering the square of the absolute value of Equation (8.12); i.e.:

$$|H(\omega)|^2 = \left(\frac{1+e^{-j\omega}}{2}\right)^K \left(\frac{1+e^{j\omega}}{2}\right)^K |Q(\omega)|^2 \tag{8.29}$$

Requiring the transfer function $H(\omega)$ to have K zeros at Nyquist frequency ($\omega = \pi$) is equivalent to requiring $|H(\omega)|^2$ to have $2K$ zeros at $\omega = \pi$. Taking into account the fact that $|H(\omega)|^2$ is the Fourier transform of autocorrelation sequence of $r_h[l]$, evaluating the $2k$th order derivative of $|H(\omega)|^2$ and making use of the symmetry property of the autocorrelation sequence $r_h[l]$, it can be easily shown that

$$\sum_{l=1}^{L-1} (-1)^l \, (l)^{2k} r_h\,[l] = 0 \quad \text{for } k = 0, 1, \ldots, K-1 \tag{8.30}$$

Equation (8.30) states the regularity constraint in terms of autocorrelation sequence $r_h[l]$.

The admissibility, paraunitary and K-regularity conditions are readily available in the auto-correlation domain (Equations (8.26), (8.28) and (8.30), respectively). Therefore, we only have to derive the objective function. Now, we know that

$$r_h[n] = \begin{cases} \sum\limits_{m=0}^{L-n-1} h[m]\; h[m+n] & n \geq 0 \\ r_h(-n) & n < 0 \end{cases} \tag{8.31}$$

and

$$\begin{aligned} r_g[n] &= \sum_{m=0}^{L-n-1} g[m]\; g[m+n] \quad \text{for } n \geq 0 \\ &= \sum_{m=0}^{L-n-1} ((-1)^m h[L-m])((-1)^{m+n} h[L-(m+n)]) \\ &= (-1)^n r_h[n] \end{aligned} \tag{8.32}$$

Applying the corollary[6]: *The sum of squares of a cross-correlation between two functions equals the inner product of the autocorrelation sequences of these two functions,* and the double shift orthogonality property:

$$[2x] = \delta[x] = \begin{cases} 1, & \text{for } x = 0 \\ 0, & \text{otherwise} \end{cases} \quad \text{where } x = 0, 1, \ldots, \left\lfloor \frac{L-1}{2} \right\rfloor \tag{8.33}$$

The cross-correlation function $r_{hg}[n]$ can be rewritten in terms of $r_h[n]$ as follows:

$$\sum_{n=0}^{L-1} |r_{hg}[n]|^2 = \sum_{n=0}^{L-1} r_h[n]\, r_g[n]$$

$$= \sum_{n=0}^{L-1} r_h[n]\,((-1)^n r_h[n]) = \underbrace{\sum_{x=0}^{(\frac{L}{2}-1)} (r_h[2x+1])^2}_{\text{Odd numbered values}} - \underbrace{\sum_{x=0}^{(\frac{L}{2}-1)} (r_h[2x])^2}_{\text{Even numbered values}} \tag{8.34}$$

$$= \sum_{n=0}^{(\frac{L}{2}-1)} (r_h[2n+1])^2 - 1$$

The new optimization problem can thus be stated as:

Minimize $\sum_{n=0}^{(\frac{L}{2}-1)} (r_h[2n+1])^2$ *subject to the wavelet constraints* (8.26), (8.28) and (8.30), i.e.,

$$\text{MINIMIZE:} \sum_{n=0}^{(\frac{L}{2}-1)} (r_h[2n+1])^2$$

$$\sum_{l=1}^{L-1} r_h\,[l] = \frac{1}{2}$$

$$\text{SUBJECTTO:}\; r_h\,[2k] = \delta[k], \quad \text{for } k = 0, 1, \ldots, \left\lfloor \frac{L-1}{2} \right\rfloor$$

$$\sum_{l=1}^{L-1} (-1)^l l^{2k} r_h\,[l] = 0, \quad \text{for } k = 0, 1, \ldots, K-1$$

[6]Proved in the Appendix.

Since the optimization problem posed above is linear it is also convex. Therefore, any linear or convex optimization tool can be used to solve this problem. In this case, we choose SeDuMi [26] as generic Semi Definite Programming (SDP) solvers to solve the optimization problem. SeDuMi stands for *self-dual minimization* as it implements a self-dual embedding technique for optimization over self-dual homogeneous cones [26]. It comes as an additional Matlab® package and can be used for linear, quadratic and semidefinite programming. Normally it requires a problem to be described in a primal standard form but with modeling languages like YALMIP (short for Yet Another LMI Parser) the optimization problems can be directly expressed in a user-friendly higher level language [27]. Thus YALMIP allows the user to concentrate on the high-level modeling without having to worry about low-level details. We have developed a filter optimization program that incorporates most of the available optimization routines for Matlab® and which relies on YALMIP to translate the problem into the standard form. From the autocorrelation sequence, the algorithm derives filter coefficients with length L having minimum phase property[7]. At the end of the design process the filter coefficients of the analysis LPF will be generated. From the analysis the low-pass-filter (LPF) $h[n]$, the high-pass-filter (HPF) $g[n]$ and the synthesis filters, LPF $h'[n]$ and HPF $g'[n]$, can be obtained through the quadrature Mirror Filter (QMF) equations. And from these set of filters the wavelets and their duals can be derived using the 2-scale Equation (3) .

8.6 Results and Analysis

In this section we present a few results to demonstrate the design procedure. As already mentioned, the main variables of the design process are the length and regularity order of the filter.

8.6.1 Frequency and Impulse Response of Designed Filter

We set the length of the filter to 20 though it is possible to design longer or shorter filters. The order of regularity chosen is 5, which is a compromise between optimization space and wavelet regularity. The impulse response of the designed optimal filter is illustrated in Figure 8.4 and numerical values of filter coefficients are given in Table 8.1. Although the optimal filter is designed in the autocorrelation domain, the minimum-phase time domain coefficients obtained satisfy all constraints mandated by the design process.

[7] We chose filters having minimum phase because they guarantee stability.

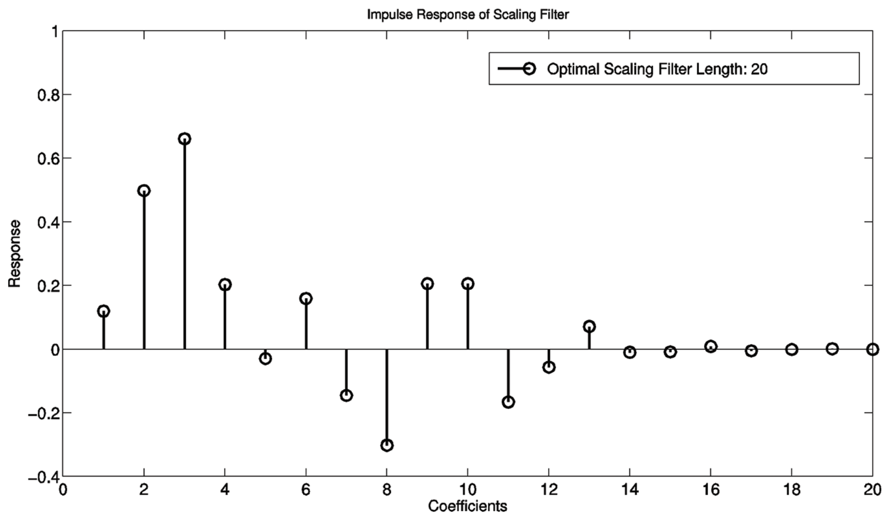

Figure 8.4 Impulse response of the optimal LPF with 20 coefficients.

Table 8.1 Optimal filter coefficients

0.119881851613898	0.498287367999060	0.660946808777660	0.203191803677134
–0.02915169068882	0.159448121842196	–0.144908809151642	–0.301681615791117
0.206305798368833	0.205999004857997	0.165410385138750	–0.0566148032177797
0.071282862607634	–0.00958254794419582	–0.0083940508446907	0.00912479119304040
–0.00498653232060	–0.00069440881953843	0.00154092796305564	–0.000370932610232259

The wavelet and scaling function of the newly designed optimal filter are illustrated in Figure 8.5a and 8.5b, respectively. The frequency response is shown in Figure 8.5c. Table 8.2 shows the specifications of the various filters used in the study along with the values of the corresponding objective functions. Clearly the designed wavelet has the lowest interference energy (due to time synchronization error).

8.6.2 Evaluation of Designed Filter under Loss of Time Synchronization

The performance of the designed wavelet is compared and contrasted with several known wavelets by means of computer simulations. We have designed a ranging/communication system with DQPSK modulation and 128 orthogonal subcarriers, corresponding to wavelet packet tree of 7 stages. Guard intervals are not used and no error estimation or correction capabilities are implemented.

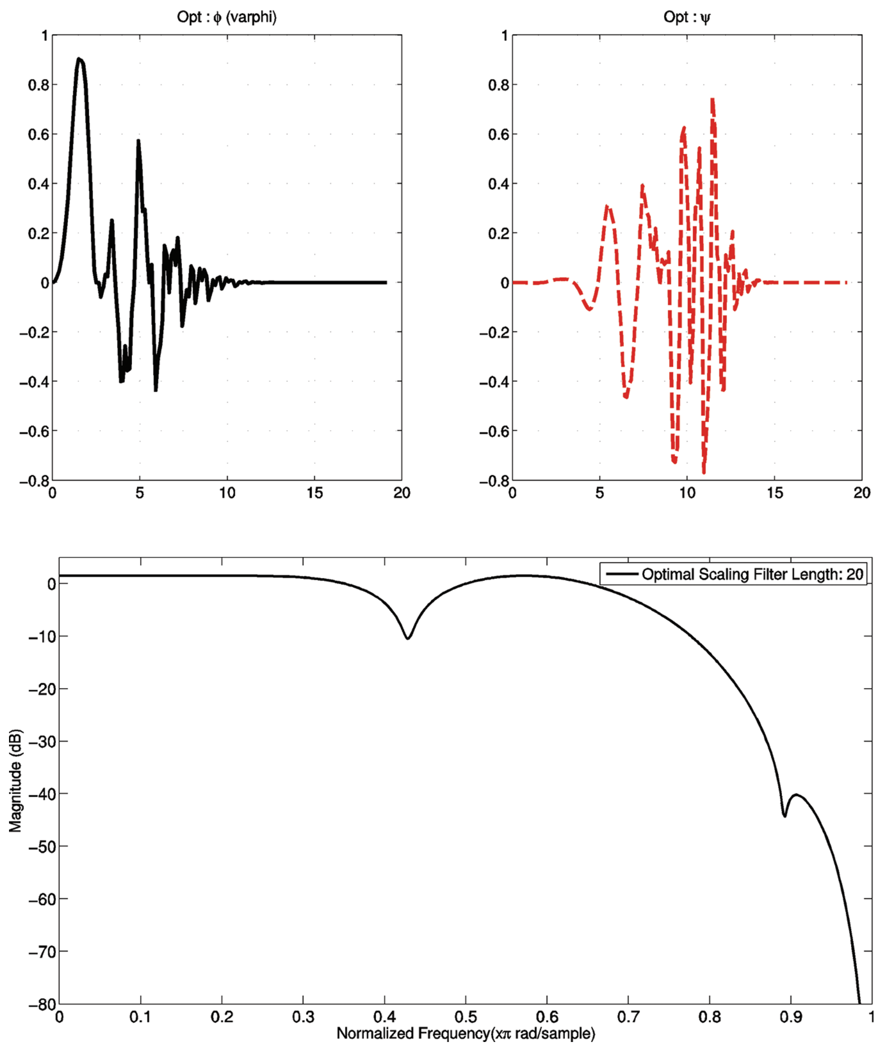

Figure 8.5 Optimal Filter; (a: top left) Scaling function, (b: top right) Wavelet function and (c: bottom) Frequency response in dB of the optimal filter.

To simplify the analysis, perfect frequency and phase synchronization are assumed. The time offset Δ_t is modeled as discrete uniform distribution between –2 and 2 samples, i.e., $\Delta_t \in [-2, -1, 0, 1, 2]$. In order to accentuate the difference in performances between various wavelets, an oversampling factor of 15 is applied. The details are tabulated in Table 8.3.

Table 8.2 Wavelet specifications and objective function

Name	Length	K-Regularity	$\sum_{n=0}^{\frac{L}{2}} (r_h[2n+1])^2$
Haar	2	1	–
Daubechies	20	10	0.41955
Symlets	20	10	0.41955
Discrete Meyer	102	1	0.45722
Coiflet	24	4	0.41343
Optimal	20	5	0.36814

Table 8.3 Simulation setup time synchronization error

	WPM
Number of Subcarriers	128
Number of Multicarrier Symbols per Frame	100
Modulation	DQPSK
Channel	AWGN
Oversampling Factor	15
Guard Band	–
Guard Interval	–
Frequency Offset	–
Phase Noise	–
Time Offset	$\Delta_t = 2$

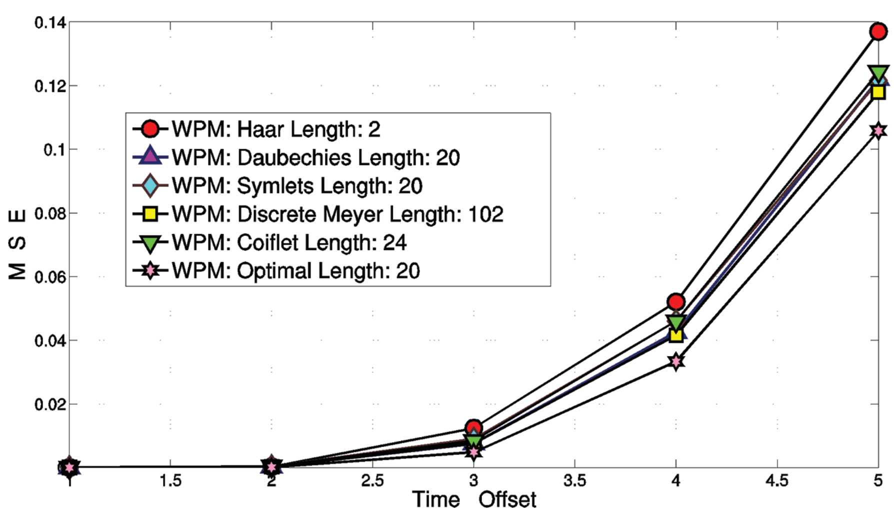

Figure 8.6 MSE of TOA estimation vs. Time Offset for WPM signal in AWGN channel (SNR = 20 dB).

The Mean Square Error (MSE) of TOA estimation is calculated for different values of time offset and is shown in Figure 8.6, respectively. Because the direction of timing error is inconsequential for WPM based system the time offset Δ_t is considered to follow a uniform distribution between 1 and 5 samples. The results presented corroborate the gains brought in by the newly designed wavelets.

8.7 Conclusions

Wavelet Packet Modulation is a strong candidate for signal design in 5G networks. It provides communication and ranging functionalities with one technology and offers enormous adaptability and flexibility to system designers. This tutorial chapter presented a methodology for designing new wavelets for communication and ranging of context-aware 5G networks when there is a time synchronization error. The design process was described as an optimization problem that accommodated the design objectives and additional constraints necessary to ensure the wavelet existence and the orthonormality. In order to obtain the global minimum, the original non-convex constraints and the objective function were translated into the autocorrelation domain. Using the new formulation, the design problem was expressed as a convex optimization problem and efficiently solved using the semi definite programming technique. To demonstrate the design mechanism for the ranging applications special filters were developed for the TOA estimation when there exists a time synchronization error. The simulation results revealed that the newly designed wavelet signal satisfied all the design objectives and outperformed the standard wavelets in terms of the MSE of TOA estimation. Importantly, the wavelet design framework presented in this chapter can easily be applied to other design criteria of 5G networks (e.g., security, spectral efficiency, throughput, latency performance, . . .) by merely altering the objective function. However, to be able to do so, the desirable properties of the wavelet bases must be translated into realizable objective functions. This can at times be challenging because the relationship between wavelet functions and filters is implicit and not direct.

References

[1] M. Benedetto, Understanding Ultra Wide Band: Radio Fundamentals, Prentice Hall PTR, NJ. 2004.
[2] M. Ghavami, L. B. Michael and R. Kohno, Ultra Wideband Signals and Systems in Communications Engineering, Wiley, 2004.

[3] Y. T. Chan, K. C. Ho, "A Simple and Efficient Estimator for Hyperbolic Location," IEEE Transactions on Signal Processing," Vol. 42, No. 8, pp. 1905–1915, Aug. 1994.
[4] H. Nikookar and R. Prasad, Introduction to Ultrawidebband for Wireless Communications, Springer, 2009.
[5] H. Nikookar, Wavelet Radio: Adaptive and Reconfigurable Wireless Systems based on Wavelets, Cambridge University Press, 2013.
[6] Daubechies, "Ten Lectures on Wavelets", Society for Industrial and Applied Mathematics, Philadelphia, Pennsylvania, 1992.
[7] P. P. Vaidyanathan, Multirate Systems and Filter Banks, Prentice Hall PTR, Englewood Cliffs, New Jersey, 1993.
[8] M. Jansen and P. Oonincx, Second Generation Wavelets and Applications, Springer, 2005.
[9] W. J. Phillips, "Wavelet and filter banks course notes", 2003 [Available Online] http://www.engmath.dal.ca/courses/engm6610/notes/notes.html
[10] M. Vetterli and I. Kovacevic, Wavelets and Subband Coding. Englewood Cliffs, New Jersey: Prentice-Hall PTR, 1995.
[11] E. L. Lawler and D. E. Wood, "Branch-and-bound methods: A survey", JSTOR Operations Research, Vol. 14, No. 4, pp. 699–719, August 1966.
[12] E. Alizadeh, "Interior point methods in semidefinite programming with applications to combinatorial optimization", SIAM Journal of Optimization, Vol. 5, pp. 13–51, 1995.
[13] Y. Ye, Interior Point Algorithms: Theory and Analysis, New York, Wiley, 1997.
[14] S. Boyd, L. El Ghaoui, E. Feron, V. Balkrishnan, "Linear matrix inequalities in system and control theory", SIAM Study in Applied Mathematics, Vol. 15, June 1994.
[15] S. Boyd, L. Vandenberghe, Convex Optimization, Cambridge University Press, 2004.
[16] L. Vandenberghe, S. Boyd, "Semidefinite programming", SIAM review, Vol. 38, No. 1, pp. 49–95. March 1998.
[17] H. Wolkowicz, R. Saigal, L. Vandenberghe, Handbook of Semidefinite Programming, Kluwer Academic Publisher, 2000.
[18] R. Hettich, K. O. Kortanek, "Semidefinite programming: Theory, methods and applications", SIAM Review, Vol. 35, No. 3, pp. 380–429, September 1993.
[19] A. Karmakar, A. Kumar, R. K. Patney, "Design of an optimal two-channel orthogonal filterbank using semidefinite programming", IEEE Signal Processing Letters, Vol. 14, No. 10, pp. 692–694, October 2007.

[20] J. Wu, K. M. Wong, “Wavelet packet division multiplexing and wavelet packed design under timing error effects”, IEEE Transaction. on Signal Processing, Vol. 45, No. 12, pp. 2877–2890, December 1997.
[21] J. K. Zhang, T. N. Davidson, K. M. Wong, “Efficient design of orthonormal wavelet bases for signal representation”, IEEE Transactions on Signal Processing, Vol. 52, No. 7, July 2007.
[22] H. Nikookar, “Signal design for context aware distributed radar sensing networks based on wavelets,” IEEE Journal of Selected Topics in Signal Processing, Vol. 9, No. 2, March 2015.
[23] B. Alkire, L. Vandenberghe, “Convex optimization problems involving finite autocorrelation sequences”, Mathematical Programming, Series A93, pp. 331–359, 2002.
[24] T. N. Davidson, L. Zhi-Quan, K. M. Wong, “Orthogonal pulse shape design via semidefinite programming”, IEEE International Conference on Acoustics, Speech and Signal Processing (ICASSP ’99), Vol. 5, pp. 2651–2654, March 1999.
[25] T. N. Davidson, L. Zhi-Quan, J. F. Sturm, “Linear matrix inequality formulation of spectral mask constraints with applications to FIR filter design”, IEEE Transaction. on Communications, Vol. 50, No. 11, pp. 2702–2715, November 1999.
[26] J. F. Sturm, “Using SeDuMi 1.02, a MATLAB toolbox for optimization over symmetric cones”, Optimization Methods and Software, Vol. 11–12, pp. 625–653, 1999. [Available Online] http://sedumi.mcmaster.ca/
[27] J. Löfberg, “A Toolbox for modeling and optimization in MATLAB”, Proceedings of the CACSD Conference, 2004. [Available Online] http://control.ee.ethz.ch/∼joloef/wiki/pmwiki.php

Appendix: Sum of squares of cross-correlation

The sum of squares of cross-correlation magnitude is related to the autocorrelation sequences of low pass filter *H* and high pass filter *G* according to the following equation:

$$\begin{aligned}\sum_{n=0}^{L-1} |r_{hg}[n]|^2 &= \sum_{n=0}^{L-1} r_h[n]\left((-1)^n r_h[n]\right) \\ &= r_h[n] \cdot r_g[n] \end{aligned} \tag{8.A1}$$

Proof

$$\begin{aligned}
\sum_n |r_{hg}(n)|^2 &= \sum_n \left(\sum_p h[p+n]\ g[p] \right)^2 \\
&= \sum_n \sum_m \sum_p h[p+n]\ g[p]\ h[m+n]\ g[m] \\
&= \sum_m \sum_p g[p]\ g[m] \sum_n^L h[p+n]\ h[m+n] \\
&= \sum_m \sum_p g[p]\ g[m] \sum_{n=m-p} h[m]\ h[2m-p] \\
&= \sum_m \sum_p r_h[m-p]\ g[p]\ g[m] \\
&= \sum_p \sum_{n=m-p} r_h[n]\ g[p]\ g[n+p] \\
&= \sum_n r_h[n]\ r_g[n] \\
&= r_h[n] \cdot r_g[n] \qquad (8.A2)
\end{aligned}$$

About the Author

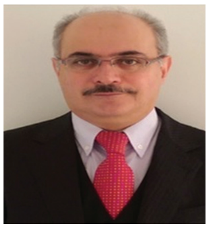

Homayoun Nikookar received his Ph.D. in Electrical Engineering from Delft University of Technology in 1995. In the past he has led the Radio Advanced Technologies and Systems (RATS) program, and supervised a team of researchers carrying out cutting-edge research in the field of advanced radio transmission. He has received several paper awards at international conferences and symposiums. Dr. Nikookar has published about 150 papers in the peer reviewed international technical journals and conferences, 12 book chapters and is author of two books: Introduction to Ultra Wideband for Wireless Communications, Springer, 2009 and Wavelet Radio, Cambridge University Press, 2013.